Faraday Discussions

Cite this: *Faraday Discuss.*, 2017, **196**, 143

PAPER

Structure–activity relationship for the solid state emission of a new family of "push–pull" π-extended chromophores†

Andrea Nitti,[a] Francesca Villafiorita-Monteleone,[b] Aurora Pacini,[a] Chiara Botta,[b] Tersilla Virgili,[c] Alessandra Forni,[d] Elena Cariati,[e] Massimo Boiocchi[f] and Dario Pasini*[a]

Received 27th June 2016, Accepted 22nd July 2016
DOI: 10.1039/c6fd00161k

We report the design, synthesis, molecular optical properties, and solid state emissive behaviour of a series of novel compounds, which, similar to the archetypal AIE luminogen tetraphenylethene, are formed of a central olefin stator and decorated with either three or four rotors. These rotors, being either electron-rich substituted benzenes, or electron-withdrawing functional groups (esters, ketones, cyano groups) confer a "push–pull" character to the overall molecular structure. Building on both new and already published contributions, a comprehensive picture of the properties and the potential of these compounds is provided.

Introduction

Strong emission in the aggregated state for organic compounds has long been considered counterintuitive: aggregation-caused quenching (ACQ) takes place in the condensed phase for most π-extended, emitting chromophores. ACQ severely inhibits their application in real-world devices, such as light-emitting diodes, optical waveguides and lasers.[1] In recent years, Tang and other groups have demonstrated that selected organic dyes can indeed behave in such

[a]*Department of Chemistry and INSTM Research Unit, University of Pavia, Viale Taramelli, 10, 27100 Pavia, Italy. E-mail: dario.pasini@unipv.it*
[b]*ISMAC-CNR, Via Corti 12, 20133 Milano, Italy*
[c]*IFN-CNR, Dipartimento di Fisica, Politecnico di Milano, Piazza Leonardo Da Vinci, 32, 20132 Milano, Italy*
[d]*ISTM – CNR, c/o Dipartimento di Chimica, Università Degli Studi di Milano, Via Venezian, 21, 20133 Milano, Italy*
[e]*Università Degli Studi di Milano, Dipartimento di Chimica, via Golgi 19, 20133 Milano, Italy*
[f]*Centro Grandi Strumenti, University of Pavia, Via Bassi, 21 – 27100 – Pavia, Italy*

† Electronic supplementary information (ESI) available: Additional graphs with molecular optical properties, tables with NMR shifts, copies of NMR spectra for new compounds. CCDC 1487807 and 1487808. For ESI and crystallographic data in CIF or other electronic format see DOI: 10.1039/c6fd00161k

a counterintuitive way: they are non-emissive when in diluted solutions, and become highly emissive in the solid state.[2]

Many molecular systems have been proven to be efficient AIE luminogens; one prototypical AIE emissive chromophore, and the first to have been reported, is hexaphenyl-substituted silole (HPS), published by Tang and coworkers in 2001.[3] Aggregation-induced emission (AIE) is frequently ascribed to restricted internal rotations (RIR):[4] for example, when HPS is in solution, the rotation of its phenyl rings dissipates the excitation energy, whereas aggregate formation in crystals does not allow the phenyl ring rotations and a radiative decay with a nanosecond lifetime is activated. Apart from silole systems, a great deal of work has been done with other AIE luminogens, aimed at confirming and exploiting the RIR principle. To date, many other families of compounds have since been proposed, featuring a variety of scaffold functionalities and different "switching on" mechanisms for emission in the solid state. The field has been recently and comprehensively reviewed.[5]

The most widely used of prototypical AIE chromophores is tetraphenylethene (TPE), which has been extensively investigated. The central olefin stator of the molecule is surrounded by four peripheral aromatic rotors (the phenyl rings). Its high solid state quantum yield, and its relatively simple synthesis have prompted its inclusion in a wide variety of complex architectures, such as linear[6] and hyperbranched polymers,[7] and metal–organic frameworks.[8] In most cases, the high solid state efficiency of the molecular scaffold is fully preserved with the introduction of the organic functionalities needed for the its covalent or non-covalent bridging to macromolecular/supramolecular architectures. In other words, the TPE scaffold is able to withhold AIE activity even if major modifications are inserted within its chemical structure.

D–π–A dyes usually exhibit unique emissive properties due to their intramolecular charge transfer (ICT) transitions, and they are of great potential interest since ground and excited electronic states can be tuned under various conditions.[9] We have serendipitously discovered a new class of AIE luminogens with a "push–pull" structure. They possess similarities to TPE, since the central stator is still a carbon–carbon double bond, which is decorated with three (not four, as in TPE) substituents, two carboxylate esters and a 4-dialkylaminophenyl branch (Fig. 1, compounds series **1**).[10] Studying one of the AIE active compounds in detail using ultrafast pump–probe spectroscopy and combining with calculations, we have given direct evidence that RIR is the key process for switching on the AIE properties.[11]

More recently, compound **2b** (Fig. 1) was effective in unravelling important features of the twisted intramolecular charge transfer mechanism, a peculiar characteristic of such "push–pull" structures.[12]

The potential of "push–pull" molecular scaffolds for the design of innovative AIE luminogens is huge, since the molecular optical properties (absorption and emission λ_{max}), and consequently the solid state emission, can in principle be tuned using "push" and "pull" substituents with variable electron-donating and electron-withdrawing characters. In fact, we have recently reported that one of these compounds (**5a** in Fig. 1) crystallizes in four different polymorphs all showing different emission colors, and that the emission color can be tuned *via* heating and grinding in the solid state, highlighting the potential application for stimuli responsive solid-state materials.[13]

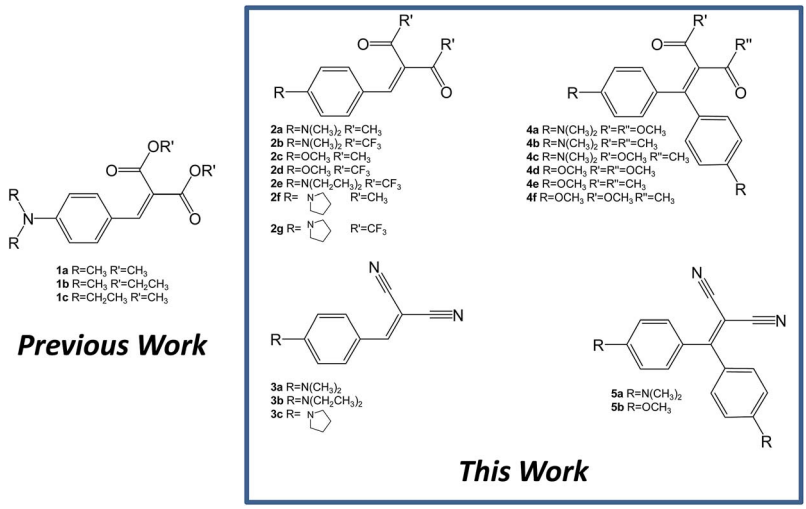

Fig. 1 Chemical structures of compound series **1–5**.

In this paper, we report our further achievements into the fine tuning of the previously proposed molecular "push–pull" structures in order to investigate their potential in terms of AIE, to match requirements for optoelectronic and sensing applications. We will discuss the optical properties and the AIE and solid state behavior of a series of compounds in which the original molecular structure has been systematically varied (Fig. 1). Together with the electronic characteristics of the rotor groups around the stator mentioned above, which are necessary to give a "push–pull" character, given the importance of the RIR mechanism, variations in the steric hindrance of the rotor functional groups around the stator have also been addressed.

Results and discussion

Design and synthesis of the molecular modules

The compounds presented and discussed in this study are shown in Fig. 1. For the sake of clarity we have divided them into five different classes (compounds **1–5**). The compounds in series **1** have been already reported, and possess ester derivatives as the "pull" components in a trisubstituted ethylene molecular scaffold; they bear minimal differences between them, either in the nature of the alkyl ester substituents, or in the nature of the dialkyl amino substituents. In the compounds in series **2**, the "pull" ester moieties have been changed to ketones and trifluoromethylketones, both possessing a similar degree of steric hindrance with respect to esters, but with substantially different electron-withdrawing characteristics, as testified by their σ_p Hammett parameters[14] (0.45 for $COOCH_3$, 0.50 for $COCH_3$, and 0.80 for $COCF_3$). Furthermore, for the compounds in series **2**, the "push" dimethylamino group has been changed in two complementary ways: (a) it has been substituted with a methoxy group, and (b) it has been changed with linear or cyclic dialkylamino groups, addressing differences in the packing properties in the solid state. The importance of the length of the dialkylamino

substituent has already been demonstrated in the compounds in series **1**, where a switching off of the AIE properties was observed on changing the dimethylamino to diethylamino "pull" moieties.[10a]

The compounds in series **3** have been designed with cyano substituents: linear functional groups with a low steric hindrance, possessing different electronic characteristics with respect to esters or ketones ($\sigma_p = 0.66$). Variable dialkylamino substituents have also been synthesized in this series. The introduction of a further dimethylaminoaryl "pull" moiety into the molecular skeleton to form tetrasubstituted ethylene, "cruciform-like" derivatives[15] has been synthetically achieved (series **4** and **5**).

The synthesis of series **2–3** was carried out following adaptations of reported procedures starting from the appropriate aldehyde and the 1,3-dicarbonyl compound or malononitrile. An initial screening of the optimal conditions was performed for the synthesis of compound **2a**, which has been previously reported. Yields using the reported procedure,[16] with piperidinium acetate as the catalyst, were somewhat disappointing (17%). Other published methods (with $CuCl_2$ as catalyst)[17] for unsubstituted benzaldehyde were equally unsatisfactory (17%), whereas the use of an excess of acetic anhydride (procedure published for the synthesis of the previously known **2d**)[18] gave improved yields (25% for **2a**). This last methodology was then applied to all compounds in series **2** and **3**, with yields ranging, after purification using column chromatography, from 25% to 76% (Scheme 1, top).

The compounds in series **4** and **5** were synthesized *via* silver triflate mediated condensation[19] of the appropriate 4,4′-disubstituted thiobenzophenone (either commercially available or *ad hoc* synthesized from the corresponding dibenzophenone with Lawesson's reagent[20]), and the appropriate 1,3-dicarbonyl compound or malononitrile (Scheme 1, bottom). Yields after purification using column chromatography ranged between 21 and 81%. All new compounds were

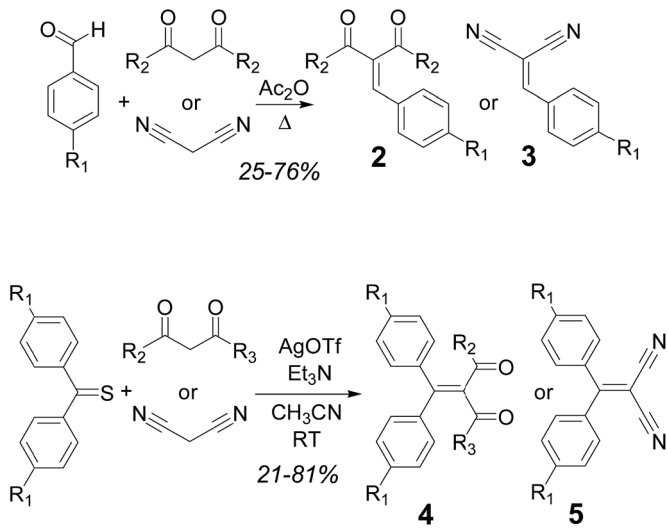

Scheme 1 Synthesis of compounds in series **2–5**.

fully characterized using NMR spectroscopy and mass spectrometric techniques. Some of the yields are rather low: however, monitoring of the reaction mixture using TLC in these cases revealed essentially a spot-to-spot conversion of the starting aldehyde or ketone into the product. It is likely, therefore, that collateral reactions between the starting material and the catalysts or reaction solvents generate byproducts, presumably removed during the work-up.

The room temperature ^{1}H NMR spectra of all the compounds showed the expected simple patterns and the presence of only one set of signals for each group of symmetry-related proton resonances, revealing that all possible dynamic processes are fast on the NMR timescale at this temperature. A comparison between the relevant signals of the ^{1}H and ^{13}C NMR spectra is presented in Tables S1–S4 of the ESI† section. No evidence of enol structures could be found in the spectra of compounds **2a** and **2c**, and **4b**, **4c**, **4e**, **4f**, which bear hydrogen atoms α to a carbonyl to thus support the possibility of enolization: signals related to the CH_3 groups integrate correctly with respect to the rest of the proton resonances, and no vinyl signals in the appropriate region (5–6 ppm) could be detected.

The locking of the rotation of the "pull" moieties (for example, the ester and ketones in compounds **1a** and **2b**, respectively) and of the aryl moiety around its own axis are both key elements responsible for the molecular rigidification and the activation of the RIR mechanism in solid-state emission.[10a,11,12] Compounds **3a** and **5a** possess linear cyano moieties, for which any lateral steric interaction is not possible as the "pull" components, and thus they can be ideal models to investigate the "pirouetting" movements of the aryl moieties. Variable temperature NMR studies performed on compound **3a** revealed that this molecular rotation becomes slow on the NMR timescale (Fig. 2) upon freezing the sample in d_8-THF. At low temperatures, the H_b protons are split into two different signals as a result of the loss of the local symmetry around the aryl main axis, and coalesce at

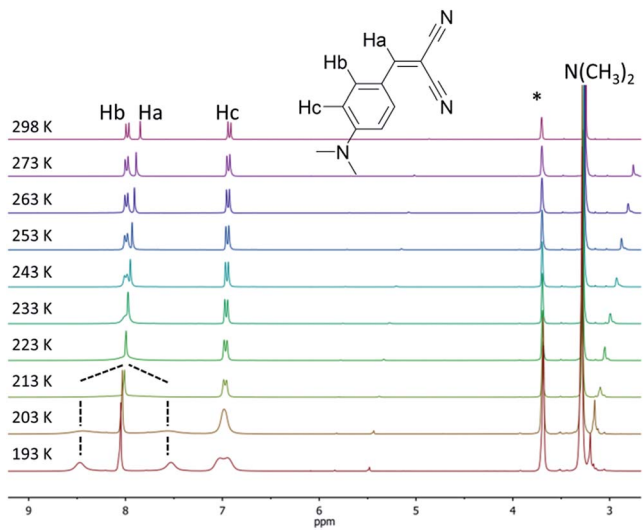

Fig. 2 Variable temperature ^{1}H NMR spectra (300 MHz, d_8-THF) of compound **3a**. The asterisk denotes residual the solvent peak.

213 K. A free energy barrier for such a dynamic process (9.6 kcal mol^{-1}) could be calculated with the coalescence method.[21]

For compound **5a**, such signal splitting could not be observed down to 193 K (Fig. S1†), meaning that a precise value for the energy barrier of the rotation of the aryl rings around their axes, to compare with **3a**, could not be calculated.

Molecular optical properties

The relevant optical properties for the compounds discussed are reported in Table 1 in order to rationalize their optical–structural relationship.

The λ_{max}, corresponding to the HOMO–LUMO energy, for a homologous series of compounds bearing the same electron-donating substituent was found to be modulated by the nature of the electron-withdrawing substituent. In fact, a linear correlation between the σ_p Hammett's parameters of the "pull" moiety (Fig. 3) and the λ_{max} for compounds **1a**, **2a**, **2b**, **3a**, all bearing dimethylamino groups, was found. Such a correlation indicates a "through bond" effect of the substituents, and demonstrates an effective conjugation through the π-systems, formally composed of a styrene-like moiety. A similar linear correlation (based on compounds **4a**, **4b** and **5a**) could be verified for cruciform-like compounds (Fig. S2†). Such correlations could also be useful in predicting the properties of analogous compounds utilizing different "push–pull" substituents. The direct comparison, where possible, between monoaryl systems (series **2** and **3**) and cruciform-like systems (series **4** and **5**) demonstrates (Table 1) that the introduction of a further aryl branch does not enhance the λ_{max} and the "push–pull" character of the system (compare for example **3a** *vs.* **5a**, and **1a** *vs.* **4a**).

Table 1 Optical properties of the compounds of series **1–5** in solution and as powders

Compound	λ_{abs}[a] (nm)	λ_{em} (nm), solution[b]	λ_{em} (nm), powder	PL QY (%), solution	PL QY (%), powder	Physical appearance
1a	378	429[c]	468	<0.1	38	Solid
1b	380	440[c]	473	<0.1	38	Solid
1c	380	445[c]	522	<0.1	1	Solid
2a	382	462	520	0.33	1	Solid
2b	461	553	625	<0.1	11	Solid
2c	274	n.a.	n.a.	n.a.	n.a.	Oil
2d	360	n.a.	n.a.	n.a.	n.a.	Oil
2e	467	528	630	<0.1	<0.1	Solid
2f	390	456	540	1	<0.1	Solid
3a	430	488	615	0.9	3	Solid
3b	436	491	550, 630	1.4	5	Solid
3c	436	491	630	0.87	3	Solid
4a	360	n.a.	n.a.	n.a.	n.a.	Oil
4b	385	495	500	<0.1	<0.1	Solid
4c	384	495	512	0.1–1	1	Solid
5a	432	511	530, 535, 595	<0.1	11[d]	Solid
5b	337	395	480	<0.1	5	Solid

[a] In MeCN solution (1–5 10^{-5} M). [b] Emission maximum, 10^{-6} M solution. [c] Data taken from ref. 10*a*, in toluene. [d] Max PL QY of the polymorphs.

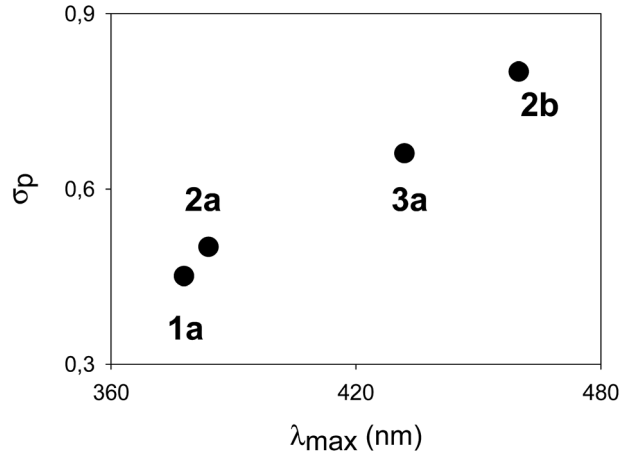

Fig. 3 Correlation between λ_{max} and σ_p Hammett's parameters for the dimethylamino-terminated compounds **1a**, **2a**, **2b** and **3a** (fitting coefficient $r^2 = 0.99$).

All the compounds reported in Table 1 show a very low PL QY in solution, which does not depend much on the polarity of the solvent. Compounds **1a**,[10a] **2b**,[12] **2e**, **3a**, **3b** and **5a**[13] show solvatochromic behaviour related to their push–pull molecular structure (see ESI†) without any relevant variation in emission intensity.

However, for compounds **1a** and **2b**, a strong increase in PL intensity on increasing the solvent viscosity has been observed,[10a,11] indicating that the rigidity of the environment, rather than its polarity, plays an important role in their emissive process. On freezing the solutions or on adding a non-solvent to the solutions, we have reported an increase in the PL intensity for compounds **1a** and **5b**.[10a,12] In diluted solutions below the solidification point of the solvent, molecular motions are blocked by the rigidified solvent. Upon adding a non-solvent at room temperature to diluted solutions, molecular aggregation into nanoparticles blocks intramolecular motion. Their AIE properties have therefore been ascribed to the commonly observed RIR effect.

As shown in Table 1, some of the compounds display a strong enhancement in PL QY in the solid state, while others maintain nearly the same low value as in solution. Compounds **1a** and **1b** display the strongest PL enhancement, the series **3** and **5** a moderate one, while in the case of series **4** and **2** (with the exception of **2b**) no relevant variation is observed in the PL intensity between solution and the solid state. Changes in the lateral alkyl chains in the "push" moieties bring about substantial changes in the AIE properties: on changing from dimethylamino to diethylamino aryl substituents the AIE behaviour is either strongly reduced (from **1a** to **1c**) or switched off (from **2b** to **2e**). In the case of **3a** (dimethylamino, already without AIE behaviour) the change to diethylamino (**3b**) confirms the absence of AIE behaviour.

Among the other compounds, **3b** and **5a** display quite interesting features with solvatochromism in solution, good solid state QYs and the presence of different components in the solid state emission, already studied in detail in the case of compound **5a**.[12] The optical absorption, PL excitation profiles (PLE)

and emission spectra of **3b** in acetonitrile solution and as powders are reported in Fig. 4. For the powder, a strong red-shift in the PL and the presence of two peaks (495 and 580 nm) in the PLE spectra are observed. The latter are very probably associated to the presence of two different species which can be separated thanks to their different solubility in pentane. Upon pentane extraction, two main contributions are observed in the emission spectrum, a shoulder at 550 nm and the main peak at 630 nm, while the insoluble portion of the powder displays a main emission at 635 nm. The relative intensity of the two contributions can be changed upon manual grinding of the powder (see ESI†).

Since, for RIR materials, the emissive properties strictly depend on the type of aggregation (crystalline *vs.* amorphous) and on the crystal rigidity, in the next section we analyse the crystal structures of the compounds in detail.

X-ray crystal structures

Crystal structures of the series **1**,[10a] and compounds **2b**[12] and **5a**[13] were previously reported by us, together with a thorough discussion, supported with DFT and TDDFT calculations,[11–13] of the structure–optical property relationships governing their emissive behaviour. It was found that their AIE properties were strictly related to their crystal structure, which is able to activate a RIR process. Moreover, by comparing the crystal structures and the solid state optical behaviours of the different compounds, we have ascribed the high PL QY (up to 38%) observed for compounds **1a** and **1b** to the formation of J-dimers.

Unlike the molecular structures of the previously reported compounds, those of series **3** (**3a**[22] and **3b**[23] being previously reported) are essentially planar. Crystals of **3c** belong to the $P\bar{1}$ space group with 6 molecules in the asymmetric unit (see Fig. 5 for its crystal packing). A subtle, not previously highlighted, feature shared by these structures, which could have some role in their emissive behaviour, was the slightly greater degree of conjugation of the

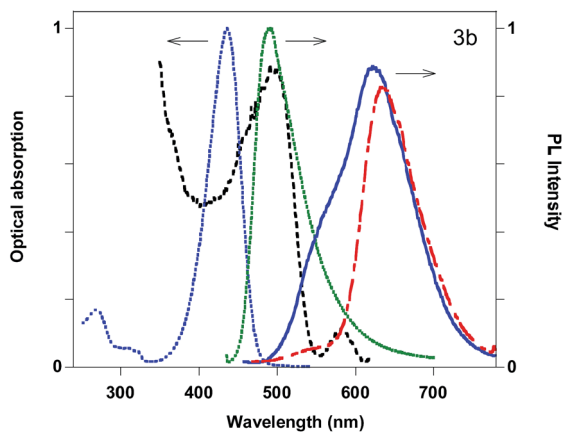

Fig. 4 Optical absorption and PL spectra of compound **3b** in acetonitrile solution (dotted lines). PLE and PL spectra of solid **3b**: pentane soluble component (solid line) and pentane insoluble component (dashed-dotted line).

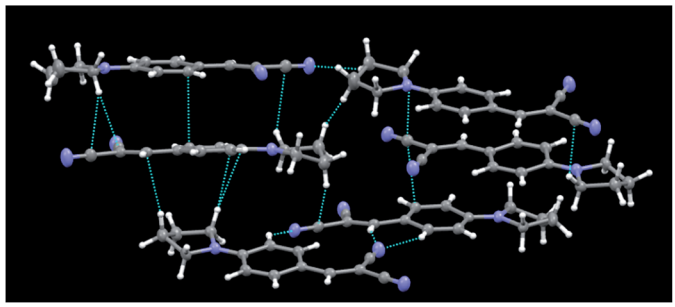

Fig. 5 Partial view of the crystal packing of **3c**, where contacts shorter than the sum of the van der Waals radii are included. Ellipsoids are drawn at the 50% probability level.

trans CN group with the benzene ring with respect to the *cis* group. The angles between the CN bond and the normal to the plane through the benzene ring were in fact 88.9(1)° (**3a**[22c]) and in the range 85.9(2)–89.5(2)° (**3c**) for the *trans* CN groups, and 79.5(1)° (**3a**) and in the range 77.6(2)–85.3(2)° for the *cis* groups. In the case of **3b**,[23b] the two angles were comparable (84.8(1) and 86.7(1)°, respectively).

The crystal structures of **3** share a pseudo layered structure, but **3a** and **3b** do not reveal the presence of significant π–π stacking interactions owing to the too long interplanar distance between adjacent benzene rings. Only C–H···N (**3a**) or C–H···N and C–H···π (**3b**) intermolecular interactions stabilize their crystal structures. In the case of **3c**, besides C–H···N and C–H···π interactions, we also observe short CC contacts (3.337 and 3.317 Å) which involve, however, only 4 of the 6 independent molecules. As a result, the presence of weak interactions in the crystal phase explains the AIE behaviour of the series of compounds **3**, while their rather low PL QY can be ascribed to the absence of strong aggregation (Fig. 5).

Crystals of **5b** belong to the *C*2/*c* space group with half a molecule in the asymmetric unit (see Fig. 6). Unlike **5a**, for which four kinds of crystals were obtained, characterized by different morphologies and absorption and

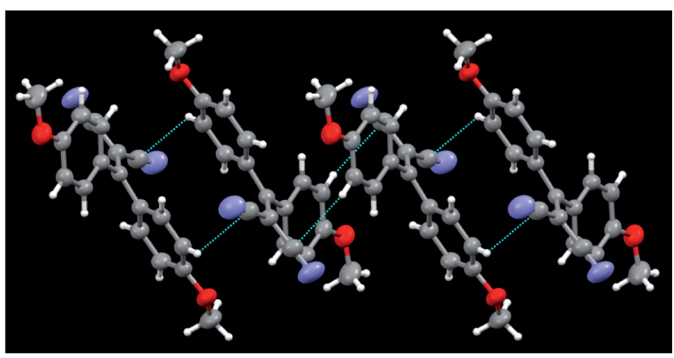

Fig. 6 Partial view of the crystal packing of **5b**, where contacts shorter than the sum of the van der Waals radii are included. Ellipsoids are drawn at the 50% probability level.

emission colours, only one phase was obtained for **5b**. A distinctive feature of these molecular structures is their twisted conformation due to the steric hindrance both between the CN and the dimethylamino-phenyl substituents and between the phenyl rings. As previously evidenced,[12] three geometrical factors can act in a concerted way to reduce such hindrance, that is, the (N)C–C=C–C(Ph) torsion angle, the reciprocal tilting of the phenyl rings (quantified through the dihedral angle between the least-squares planes through the phenyl carbon atoms) and the central double bond, which in the present structures is significantly elongated with respect to the value of 1.331(9) Å reported for (C_2)–C=C–(C_2) unconjugated bonds,[24] denoting a high degree of conjugation. It is to be pointed out that, owing to their cross-conjugated architecture,[25] the phenyl rings, connected with each other *via* two single bonds, are separately conjugated to each CN group, as well as the CN groups being separately conjugated to each phenyl ring. The conformational differences observed in the four crystals of **5a**, though small, were found to be associated with a different degree of conjugation between the molecular moieties connected through the C=C double bond. In particular, the lower the dihedral angle between the phenyl rings, the larger the distortion around the double bond and the greater the cross-conjugation. In the case of **5b**, we observe a large dihedral angle between the phenyl rings (71.6(1) *vs.* 71.8(1)–58.0(1)° found in **5a**), a lower (N)C–C=C–C(Ph) torsion angle (9.0(1) *vs.* 11.8(1)–19.9(1)° of **5a**) and a shorter C=C bond length with respect to **5a** (1.366(3) *vs.* 1.376(3)–1.390(2) Å). All these features indicate a lower cross-conjugation for **5b** with respect to **5a**.

The twisted conformations of compounds **5a** and **5b** rule out the presence of strong intermolecular π–π stacking interactions, excluding the formation of H- or J-aggregates. On the other hand, as noted for the series of compounds **3**, the weak C–H···N and C–H···π intermolecular interactions found in the structures of **5a** and **5b** are enough to fix the molecular conformations in the crystal structures to activate the RIR mechanism. In both series of compounds **3** and **5**, the absence of strong intermolecular interactions and the conformational freedom associated with the presence of several single bonds explain the formation of different polymorphs, as demonstrated from X-ray investigation for **5a** and suggested from spectroscopic evidence for **3b**.

Pump–probe experiments

A deep understanding of the role of the intramolecular torsional mobility in AIE molecules is of crucial importance in order to design new organic compounds with improved optoelectronic properties. We reported the spectral evolution of the stimulated emission of the series of compounds **1** dissolved in solution, showing that the torsional relaxation toward the equilibrium geometry of the excited state takes place on a time scale that depends on the solvent viscosity.[11] Pump–probe ultrafast dynamics have also been employed to study the time evolution of the excited states of compound **2b**, whose long-living optical gain was detected only when the twisted intramolecular charge transfer mechanism is inhibited on increasing the solvent viscosity.[12]

Here we report ultrafast pump–probe measurements on two solutions of compound **5a** displaying different viscosities, namely polyethylene glycol (PEG)

and acetonitrile (ACN). In this way it is possible to temporally resolve the spectral evolution of the excited states created after the pump excitation of the molecule dispersed in viscous and non-viscous solvents.

In this experiment, the transmission of a white light pulse (probe) is detected at different time delays with respect to the pump excitation (400 nm). The differential transmission spectra of the probe pulse $\Delta T/T$ (where $\Delta T = T_{on} - T$, and T_{on} is the transmission of the probe light with pump excitation and T is the transmission of the probe light without pump excitation) taken at different probe delays is then obtained. A positive $\Delta T/T$ signal (transmission increasing after pump excitation) is an indication of bleaching of the ground state when the signal spectrally overlaps the absorption spectrum, or of Stimulated Emission (SE) from the excited state when the signal overlaps the PL spectrum of the molecule. The time-resolved spectra (Fig. 7) recorded in both solvents show a positive broad band that can be associated with Stimulated Emission (SE peak at around 530 nm). In ACN solution after around 1 ps the formation of a negative Photoinduced Absorption (PA) band centered at 520 nm is observed, showing a fast decay on a time scale of a few ps (red line, inset Fig. 7, top panel). On the contrary, in PEG solution there is no formation of a PA band in this time (black line, inset Fig. 7, top panel).

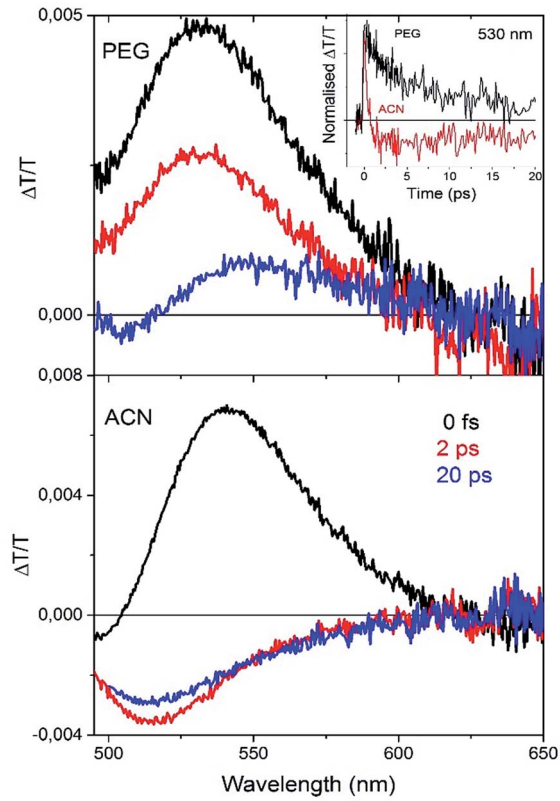

Fig. 7 Differential transmission spectra at 0 fs (black line), 2 ps (red line) and 20 ps (blue line) probe delays for PEG (top panel) and ACN (bottom panel) solutions. Dynamics at 530 nm are shown for both solutions in the inset of the top panel.

Conclusions

We have reported and compared the design, synthesis, molecular optical properties, and solid state emissive behaviour of several series of novel compounds with "push–pull" character. The compounds bear three or four substituents around a central olefin stator. While all the structures are non-emissive in solution, a handful of them possess solid-state emission with quantum yields over 10%. With the exception of compound **5a**, all AIE compounds are characterized by having three substituents around the stator. As a general trend, the use of 4-methoxyaryl substituents as the "push" component does not bring any useful solid-state emissive behavior.

Our classes of compounds are efficient in terms of tunability of emission response, but the translation of molecular design into efficient solid state emission is far from straightforward. The nice correlations with Hammett's parameters demonstrate the possibility of predicting and rationally tuning the energy gaps of these structures. However, good solid state emission is activated or deactivated with subtle changes in the molecular structures, sometimes in unpredictable ways. As such, the potential incorporation of the most promising of the structures presented here into complex covalent scaffolds (polymers, covalent organic frameworks) for functional applications cannot at present be considered immediately as occurs with other AIE scaffolds.

Experimental

General experimental for synthesis

All available compounds were purchased from commercial sources and used as received. Compounds **2b**[12] and **5a**[13] were previously reported by us. THF (Na, benzophenone), Et_2O (Na, benzophenone) and CH_2Cl_2 (CaH_2) were dried and distilled before use. ^1H and ^{13}C NMR spectra were recorded from solutions of $CDCl_3$ on a Bruker 200 or AMX300 with the solvent residual proton signal as a standard. Analytical thin layer chromatography was performed on silica gel, chromophore loaded, commercially available plates. Flash chromatography was carried out using silica gel (pore size 60 Å, 230–400 mesh). ^1H and ^{13}C NMR spectra were recorded from solutions of $CDCl_3$ on 200, 300 or 500 MHz spectrometers with the solvent residual proton signal or tetramethylsilane as a standard. Mass spectra were recorded using an electrospray ionization instrument (ESI). Melting points are uncorrected.

General procedure for the synthesis of series 2 and 3

A solution of the appropriate aldehyde (1 equiv.) and ketone or malononitrile (1 equiv.) in Ac_2O (5–10 mL) was heated under reflux (140 °C) for 18 h. After cooling to room temperature, the reaction mixture was poured into water/ice, and the aqueous suspension extracted with CH_2Cl_2. The organic phase was washed with a saturated solution of $NaHCO_3$ and then dried (Na_2SO_4). The product was isolated after purification using column chromatography.

Compound 2a. From 4-dimethylaminobenzaldehyde (1.5 g, 10 mmol) and 2,4-pentanedione (1 mL, 10 mmol). Purified with column chromatography (SiO_2; hexane : AcOEt = 7 : 3) and obtained as a yellow-orange solid (572 mg, 25%).

$R_f = 0.3$ (hexane : AcOEt = 7 : 3). ^{1}H NMR ($CDCl_3$, 200 MHz, 25 °C) $\delta = 7.40$ (s, 1H; vinyl C*H*), 7.31 (d, 2H; $J = 9$ Hz, Ar*H*), 6.65 (d, 2H; $J = 9$ Hz, Ar*H*), 3.05 (s, 6H; –N(CH_3)$_2$), 2.39 (s, 3H; –COCH_3), 2.37 (s, 3H; –COCH_3). ^{13}C NMR ($CDCl_3$, 75 MHz, 25 °C) $\delta = 207.0$ (C_q), 196.3 (C_q), 151.8 (C_q), 140.9 (vinyl C_H), 137.8 (C_q), 132.2 (Ar CH), 120.1 (C_q), 111.8 (Ar CH), 40.0 (N(CH_3)$_2$), 31.6 (CH_3), 26.1 (CH_3). MS-ESI *m*/*z* (%) = 232 $[M + H]^+$ (100), 485 $[2M + Na]^+$ (70). The crystal structure of this compound has been previously reported.[26] The ^{1}H and ^{13}C NMR spectra matched those previously reported.[27]

Compound 2c. From 4-methoxybenzaldehyde (610 μL, 5 mmol) and 2,4-pentanedione (516 μL, 5 mmol). Purified with column chromatography (SiO_2; hexane : AcOEt = 9 : 1) and obtained as a yellow oil (255 mg, 25%). $R_f = 0.14$ (hexane : AcOEt = 9 : 1). ^{1}H NMR ($CDCl_3$, 200 MHz, 25 °C) $\delta = 7.63$ (s, 1H; vinyl C*H*), 7.47 (d, 2H; $J = 9$ Hz, Ar*H*), 6.93 (d, 2H; $J = 9$ Hz; Ar*H*), 3.83 (s, 3H; –OCH_3), 2.12 (m, 6H; 2CH_3). The ^{1}H NMR spectrum matched that previously reported.[28]

Compound 2d. From 4-methoxybenzaldehyde (1.2 mL, 10 mmol) and hexafluoroacetylacetone (1.4 mL, 10 mmol). Purified with column chromatography (SiO_2; hexane : CH_2Cl_2 = 7 : 3) and obtained as a yellow oil (925 mg, 28%). $R_f = 0.3$ (hexane : CH_2Cl_2 = 7 : 3). ^{1}H NMR ($CDCl_3$, 200 MHz, 25 °C) $\delta = 7.99$ (s, 1H; vinyl C*H*), 7.42 (d, 2H; $J = 9$ Hz; Ar*H*), 6.97 (d, 2H; $J = 9$ Hz; Ar*H*), 3.87 (s, 3H; –OCH_3). This compound was previously reported, but no NMR information was given.[18]

Compound 2e. From 4-diethylaminobenzaldehyde (177.3 mg, 1 mmol) and hexafluoroacetylacetone (142 μL, 1 mmol). Purified with column chromatography (SiO_2; hexane : CH_2Cl_2 = 1 : 1) and obtained as a pink waxy solid (185 mg, 50%). $R_f = 0.5$ (hexane : CH_2Cl_2 = 1 : 1). Mp = 60–62 °C. ^{1}H NMR ($CDCl_3$, 200 MHz, 25 °C) $\delta = 7.83$ (s, 1H; vinyl C*H*), 7.34 (d, 2H; $J = 9$ Hz; Ar*H*), 6.65 (d, 2H; $J = 9$ Hz; Ar*H*), 3.48 (q, 4H; $J = 7$ Hz; 2CH_2), 1.25 (t, 6H; $J = 7$ Hz; 2CH_3).

Compound 2f. From 4-pyrrolidinobenzaldehyde (876 mg, 5 mmol) and 2,4-pentanedione (501 mg, 5 mmol). Purified with column chromatography (SiO_2; hexane : AcOEt = 8 : 2) and obtained as an orange-brown solid (421 mg, 37%). $R_f = 0.3$ (hexane : AcOEt = 8 : 2). ^{1}H NMR ($CDCl_3$, 200 MHz, 25 °C) $\delta = 7.40$ (s, 1H; vinyl C*H*), 7.30 (d, 2H; $J = 9$ Hz; Ar*H*), 6.52 (d, 2H; $J = 9$ Hz; Ar*H*), 3.36 (m, 4H; 2CH_2), 2.38 (s, 3H; CH_3), 2.37 (s, 3H; CH_3), 2.04 (m, 4H; 2CH_2). ^{13}C NMR ($CDCl_3$, 75 MHz, 25 °C) $\delta = 207.2$ (C_q; –CO), 196.1 (C_q; –CO), 149.4 (C_q), 141.3 (CH), 137.1 (C_q), 132.4 (CH), 119.3 (C_q), 111.7 (CH), 47.4 (CH_2), 31.6 (CH_3), 26.1 (CH_3), 25.3 (CH_2).

Compound 2g. From 4-pyrrolidinobenzaldehyde (876 mg, 5 mmol) and hexafluoroacetylacetone (700 μL, 5 mmol). Purified with column chromatography (SiO_2; hexane : CH_2Cl_2 = 1 : 1) and obtained as a dark red solid (512 mg, 28%). $R_f = 0.4$ (hexane : CH_2Cl_2 = 1 : 1). Mp = 89–91 °C. ^{1}H NMR ($CDCl_3$, 200 MHz, 25 °C) $\delta = 7.85$ (s, 1H; vinyl C*H*), 7.35 (d, 2H; $J = 9$ Hz; Ar*H*), 6.45 (d, 2H; $J = 9$ Hz; ArH), 3.45 (t, 4H; 2CH_2), 2.08 (m, 4H; 2CH_2). ^{13}C NMR ($CDCl_3$, 75 MHz, 25 °C) $\delta =$ 187.6 (q, C_q; $J = 35$ Hz), 177.5 (q, C_q; $J = 35$ Hz), 152.1 (C_q), 151.8 (CH), 135.2 (CH), 119.2 (C_q), 118.1 (C_q), 117.1 (q, C_q; $J = 300$ Hz), 115.3 (q, C_q; $J = 300$ Hz), 112.4 (CH), 47.8 (CH_2), 25.2 (CH_2).

Compound 3a. From 4-dimethylaminobenzaldehyde (746 mg, 5 mmol) and malononitrile (330 mg, 5 mmol). Purified with column chromatography (SiO_2; hexane : CH_2Cl_2 = 2 : 8) and obtained as an orange solid (388 mg, 40%). $R_f = 0.7$ (hexane : CH_2Cl_2 = 2 : 8). ^{1}H NMR ($CDCl_3$, 200 MHz, 25 °C) $\delta = 7.83$ (d, 2H; $J = 9$ Hz; Ar*H*), 7.48 (s, 1H; vinyl C*H*), 6.68 (d, 2H; $J = 9$ Hz; Ar*H*), 3.15 (s, 6H; –N(CH_3)$_2$). ^{13}C NMR ($CDCl_3$, 75 MHz, 25 °C) $\delta = 157.9$ (CH), 154.1 (C_q), 133.7 (CH), 119.2 (C_q),

115.9 (C_q; –CN), 114.8 (C_q; –CN), 111.5 (CH), 71.9 (C_q), 40.0 (CH_3). The ^{1}H NMR spectrum matched the one previously reported.[29]

Compound 3b. From 4-diethylaminobenzaldehyde (886 mg, 5 mmol) and malononitrile (330 mg, 5 mmol). Purified with column chromatography (SiO_2; hexane : CH_2Cl_2 = 2 : 8) and obtained as a dark pink solid (851 mg, 76%). R_f = 0.4 (hexane : CH_2Cl_2 = 2 : 8). ^{1}H NMR ($CDCl_3$, 200 MHz, 25 °C) δ = 7.81 (d, 2H; J = 9 Hz; Ar*H*), 7.44 (s, 1H; vinyl C*H*), 6.68 (d, 2H; J = 9 Hz; Ar*H*), 3.48 (q, 4H; J = 7 Hz; 2CH_2), 1.25 (t, 6H; J = 7 Hz; 2CH_3). ^{13}C NMR ($CDCl_3$, 75 MHz, 25 °C) δ = 157.7 (CH), 152.3 (C_q), 134.0 (CH), 118.8 (C_q), 116.1 (C_q; –CN), 114.9 (C_q; –CN), 111.2 (CH), 71.0 (C_q), 44.8 (CH_2), 12.4 (CH_3). The ^{1}H and ^{13}C NMR spectra matched those previously reported.[30] The crystal structure of this compound has been previously reported.[23b]

Compound 3c. From 4-pyrrolidinobenzaldehyde (876 mg, 5 mmol) and malononitrile (330 mg, 5 mmol). Purified with column chromatography (SiO_2; hexane : CH_2Cl_2 = 2 : 8) and obtained as a brown-orange solid (316 mg, 29%). R_f = 0.55 (hexane : CH_2Cl_2 = 2 : 8). ^{1}H NMR ($CDCl_3$, 200 MHz, 25 °C) δ = 7.80 (d, 2H; J = 9 Hz; Ar*H*), 7.44 (s, 1H; vinyl C*H*), 6.57 (d, 2H; J = 9 Hz; Ar*H*), 3.45 (m, 4H; 2CH_2), 2.09 (m, 4H; 2CH_2). ^{13}C NMR ($CDCl_3$, 75 MHz, 25 °C) δ = 157.9 (CH), 151.8 (C_q), 133.9 (CH), 119.0 (C_q), 116.1 (C_q), 115.1 (C_q), 111.9 (CH), 70.9 (C_q), 47.8 (CH_2), 25.2 (CH_2). This compound was previously reported.[31]

General procedure for the synthesis of series 4 and 5

Preliminary step for compounds 4d–f and 5b. A solution of 4,4′-dimethoxybenzofenone (1 equiv.) and Lawesson's reagent (1.5 equiv.) in dry toluene (30 mL) was heated to reflux (110 °C) with a Dean–Stark apparatus for 18 h. The intermediate thioketone was purified using column chromatography, then used without further characterization.

Second step for all compounds in series 4 and 5. A solution of the isolated or commercially-available thioketone (1 equiv.), the appropriate 1,3-dicarbonyl compound or malononitrile (1.2 equiv.), Et_3N (3.6 equiv.) and $AgOCOCF_3$ (2.5 equiv.) in dry CH_3CN (6 mL) was stirred in the dark at room temperature for 18 h. The solvent and base were removed *in vacuo*, and the residue partitioned between brine and AcOEt. The organic phase was then dried (Na_2SO_4) and the product was isolated after purification with column chromatography.

Compound 4a. From 4,4′-bis(dimethylamino)thiobenzofenone (284 mg, 1 mmol), malonic acid methyl ester (137 μL, 1.2 mmol), Et_3N (500 μL, 3.6 mmol) and $AgOCOCF_3$ (642 mg, 2.5 mmol) in dry CH_3CN (6 mL). Purified with column chromatography (SiO_2; hexane : AcOEt = 8 : 2) and obtained as a brown oil (89 mg, 23%). R_f = 0.1 (hexane : AcOEt = 8 : 2). ^{1}H NMR ($CDCl_3$, 200 MHz, 25 °C) δ = 7.12 (d, 4H; J = 9 Hz; Ar*H*), 6.54 (d, 4H; J = 9 Hz; Ar*H*), 3.76 (s, 6H; –OCH_3), 2.85 (s, 12H; –N(CH_3)$_2$). ^{13}C NMR ($CDCl_3$, 75 MHz, 25 °C) δ = 168.0 (C_q; CO), 158.9 (C_q), 151.0 (C_q), 131.5 (C_q), 127.9 (CH), 118.8 (C_q), 111.6 (CH), 51.8 (OCH_3), 40.1 (N(CH_3)$_2$).

Compound 4b. From 4,4′-bis(dimethylamino)thiobenzofenone (284 mg, 1 mmol), 2,4-pentanedione (123 μL, 1.2 mmol), Et_3N (500 μL, 3.6 mmol) and $AgOCOCF_3$ (642 mg, 2.5 mmol) in dry CH_3CN (6 mL). Purified with column chromatography (SiO_2; CH_2Cl_2 : AcOEt = 9 : 1) and obtained as a green emerald solid (109 mg, 31%). R_f = 0.4 (CH_2Cl_2 : AcOEt = 9 : 1). ^{1}H NMR ($CDCl_3$, 200 MHz,

25 °C) δ = 7.07 (d, 4H; J = 9 Hz; Ar*H*), 6.65 (d, 4H; J = 9 Hz; Ar*H*), 3.03 (s, 12H; –N(CH_3)$_2$), 1.92 (s, 6H; 2COOCH_3). ^{13}C NMR ($CDCl_3$, 75 MHz, 25 °C) δ = 204.5 (C_q; CO), 154.7 (C_q), 151.6 (C_q), 132.5 (C_q), 127.4 (CH), 126.3 (C_q), 111.4 (CH), 40.1 (N(CH_3)$_2$), 31.1 (CH_3). MS-ESI m/z (%) = 351 $[M + H]^+$ (100), 723 $[2M + Na]^+$ (40).

Compound 4c. From 4,4′-bis(dimethylamino)thiobenzofenone (284 mg, 1 mmol), acetoacetic acid methyl ester (139 mg, 1.2 mmol), Et_3N (500 μL, 3.6 mmol) and $AgOCOCF_3$ (642 mg, 2.5 mmol) in dry CH_3CN (6 mL). Purified with column chromatography (SiO_2; hexane : AcOEt = 8 : 2) and obtained as a yellow solid (190 mg, 52%). R_f = 0.2 (hexane : AcOEt = 8 : 2). ^{1}H NMR ($CDCl_3$, 200 MHz, 25 °C) δ = 7.08 (m, 4H; Ar*H*), 6.63 (m, 4H; Ar*H*), 3.62 (s, 3H; –OCH_3), 3.01 (m, 12H; 2N(CH_3)$_2$), 1.88 (s, 3H; CH_3). ^{13}C NMR ($CDCl_3$, 75 MHz, 25 °C) δ = 201.6 (C_q; CO), 169.5 (C_q; $COCH_3$), 156.9 (C_q), 151.7 (C_q), 132.6 (C_q), 131.6 (CH), 127.1 (C_q), 111.1 (CH), 51.7 (OCH_3), 40.0 (2N(CH_3)$_2$), 30.2 (CH_3). MS-ESI m/z = 367 $[M + H]^+$ (100), 755 $[2M + Na]^+$ (70).

Compound 4d. From 4,4′-dimethoxybenzofenone (100 mg, 0.4 mmol) and Lawesson's reagent (243 mg, 0.6 mmol); then 4,4′-dimethoxythiobenzofenone (1 equiv.), malonic acid methyl ester (1.2 equiv.), Et_3N (3.6 equiv.) and $AgOCOCF_3$ (2.5 equiv.) in dry CH_3CN (6 mL). Purified with column chromatography (SiO_2; hexane : AcOEt = 8 : 2) and obtained as a white solid (26 mg, 21%). R_f = 0.2 (hexane : AcOEt = 8 : 2). ^{1}H NMR ($CDCl_3$, 200 MHz, 25 °C) δ = 7.12 (d, 2H; J = 9 Hz; Ar*H*), 6.88 (d, 2H; J = 9 Hz; Ar*H*), 3.84 (s, 6H; –2OCH_3), 1.93 (s, 6H; 2CH_3). ^{13}C NMR ($CDCl_3$, 75 MHz, 25 °C) δ = 204.0 (C_q; CO), 161.1 (C_q), 150.3 (C_q), 141.3 (C_q), 131.9 (CH), 113.96 (CH), 55.3 (OCH_3), 31.1 (CH_3). The compound has been previously reported.[32]

Compound 4e. From 4,4′-dimethoxybenzofenone (100 mg, 0.4 mmol) and Lawesson's reagent (243 mg, 0.6 mmol); then 4,4′-dimethoxythiobenzofenone (1 equiv.), 2,4-pentanedione (1.2 equiv.), Et_3N (3.6 equiv.) and $AgOCOCF_3$ (2.5 equiv.) in dry CH_3CN (6 mL). Purified with column chromatography (SiO_2; hexane : AcOEt = 8 : 2) and obtained as a white solid (26 mg, 21%). R_f = 0.2 (hexane : AcOEt = 8 : 2). ^{1}H NMR ($CDCl_3$, 200 MHz, 25 °C) δ = 7.12 (d, 2H; J = 9 Hz; Ar*H*), 6.88 (d, 2H; J = 9 Hz; Ar*H*), 3.84 (s, 6H; –2OCH_3), 1.93 (s, 6H; 2CH_3). ^{13}C NMR ($CDCl_3$, 75 MHz, 25 °C) δ = 204.0 (C_q; CO), 161.1 (C_q), 150.3 (C_q), 141.3 (C_q), 131.9 (CH), 113.9 (CH), 55.3 (OCH_3), 31.1 (CH_3).

Compound 4f. From 4,4′-dimethoxybenzofenone (200 mg, 0.8 mmol) and Lawesson's reagent (501 mg, 1.2 mmol); then 4,4′-dimethoxythiobenzofenone (1 equiv.), acetoacetic acid methyl ester (1.2 equiv.), Et_3N (3.6 equiv.) and $AgOCOCF_3$ (2.5 equiv.) in dry CH_3CN (6 mL). Purified with column chromatography (SiO_2; hexane : AcOEt = 8 : 2) and obtained as a white solid (60 mg, 34%). R_f = 0.5 (hexane : AcOEt = 8 : 2). ^{1}H NMR ($CDCl_3$, 200 MHz, 25 °C) δ = 7.12 (m, 4H; Ar*H*), 6.86 (m, 4H; Ar*H*), 3.88 (m, 6H; –ArOCH_3), 3.61 (s, 3H; COOCH_3), 1.93 (s, 3H; CH_3). ^{13}C NMR ($CDCl_3$, 75 MHz, 25 °C) δ = 201.3 (C_q; CO), 168.2 (C_q; $COOCH_3$), 160.7 (C_q), 153.6 (C_q), 132.4 (C_q), 131.9 (CH), 131.8 (C_q), 113.9 (CH), 55.3 (OCH_3), 51.9 (OCH_3), 30.3 (CH_3). MS-ESI m/z = 340 $[M]^+$.

Compound 5b. From 4,4′-dimethoxybenzofenone (200 mg, 0.8 mmol) and Lawesson's reagent (501 mg, 1.2 mmol); then 4,4′-dimethoxythiobenzofenone (1 equiv.), malononitrile (1.2 equiv.), Et_3N (3.6 equiv.) and $AgOCOCF_3$ (2.5 equiv.) in dry CH_3CN (6 mL). Purified with column chromatography (SiO_2; hexane : AcOEt = 8 : 2) and obtained as a white solid (77 mg, 47%). R_f = 0.2 (hexane : AcOEt = 8 : 2). ^{1}H NMR ($CDCl_3$, 200 MHz, 25 °C) δ = 7.43 (d, 2H; J = 9 Hz; Ar*H*), 6.98 (d, 2H; J = 9 Hz; Ar*H*), 3.89 (s, 6H; –2OCH_3). ^{13}C NMR ($CDCl_3$, 75 MHz, 25 °C) δ = 173.8 (C_q),

163.3 (C_q), 132.9 (CH), 128.3 (C_q), 114.9 (CN), 114.1 (CH), 77.4 (C_q), 55.5 (OCH_3). The compound has been previously reported.[33]

Spectroscopical measurements

UV-Vis absorption spectra were obtained with a Perkin Elmer Lambda 900 spectrometer and PL spectra with a SPEX 270 M monochromator equipped with a N_2 cooled charge-coupled device exciting with a monochromated 450 W Xe lamp. Spectra were corrected for the instrument response. Photoluminescence quantum yields (PL QYs) of solutions were obtained using quinine sulfate or coumarine 153 as a standard. The PL QYs of solid state samples were obtained using a home-made integrating sphere, as previously reported.[34]

X-ray crystal structures

Single crystals of **3c** suitable for X-ray analysis were obtained using CH_2Cl_2/pentane. Diffraction data were collected on a Bruker Smart Apex II CCD area detector using graphite monochromated Mo-Kα radiation. Data reduction was made using SAINT programs; absorption corrections based on multiscans were obtained using SADABS.[35] The structures were solved using SHELXS-97 and refined on F^2 by full-matrix least-squares using SHELXL-14.[36] All the non-hydrogen atoms were refined anisotropically, hydrogen atoms were included as 'riding' and not refined. Crystal data and results of the refinement: orange prism 0.35 × 0.27 × 0.25 mm, $C_{14}H_{13}N_3$, $M_r = 223.27$; triclinic, $P\bar{1}$; $a = 10.8613(6)$ Å, $b = 13.0319(7)$ Å, $c = 26.5818(15)$ Å, $\alpha = 89.750(1)^\circ$, $\beta = 82.163(1)^\circ$, $\gamma = 72.238(1)^\circ$, $V = 3546.9(3)$ Å^3; $Z = 12$; $T = 120(2)$ K; μ(Mo) = 0.077 mm^{-1}. 58 049 measured reflections, 15 850 independent reflections, 11 640 reflections with $I > 2\sigma(I)$, $1.55 < 2\theta < 54.54^\circ$, $R_{int} = 0.0386$. Refinement on 15 850 reflections, 928 parameters. Final $R = 0.0642$, w$R = 0.1649$ for data with $F^2 > 2\sigma(F^2)$, $S = 1.071$, $(\Delta/\sigma)_{max} = 0.001$, $\Delta\rho_{max} = 0.668$, $\Delta\rho_{min} = -0.462$ e Å^{-3}.

Single crystals of **5b** suitable for X-ray analysis were obtained *via* slow evaporation from a $CHCl_3$ solution. Diffraction data were collected on a conventional Enraf-Nonius CAD4 four circle diffractometer, working at ambient temperature with graphite monochromated Mo-Kα Mo Kα X-radiation ($\lambda = 0.7107$ Å). Data reduction was performed with the WinGX package.[37] Absorption effects were evaluated with the ψ-scan method[38] and absorption correction was applied to the data. The crystal structure was solved by direct methods (SIR 97)[39] and refined by full-matrix least-squares procedures on F^2 using all reflections (SHELXL-14).[36] Anisotropic displacement parameters were refined for all non-hydrogen atoms; hydrogens were placed at calculated positions with the appropriate AFIX instructions and refined using a riding model. Crystal data and results of the refinement: prism 0.75 × 0.55 × 0.2 mm, $C_{18}H_{14}N_2O_2$, $M_r = 290.31$; monoclinic, $C2/c$; $a = 17.518(4)$ Å, $b = 8.666(2)$ Å, $c = 10.772(3)$ Å, $\beta = 110.164(5)^\circ$, $V = 1535.1(6)$ Å^3; $Z = 4$; $T = 293(2)$ K; μ(Mo) = 0.083 mm^{-1}. 2340 measured reflections, 2234 independent reflections, 1378 reflections with $I > 2\sigma(I)$, $4.96 < 2\theta < 59.96^\circ$, $R_{int} = 0.0182$. Refinement on 2234 reflections, 129 parameters. Final $R = 0.0491$, w$R = 0.1127$ for data with $F^2 > 2\sigma(F^2)$, $S = 1.007$, $(\Delta/\sigma)_{max} = 0.000$, $\Delta\rho_{max} = 0.170$, $\Delta\rho_{min} = -0.175$ e Å^{-3}.†

Pump–probe experiments

Time-resolved measurements were performed using a home-built femtosecond pump–probe setup. A Ti:sapphire regenerative amplifier (Libra, Coherent) was

used as a laser source, delivering 100 fs pulses at a central wavelength of 800 nm with a 4 mJ pulse energy at a repetition rate of 1 kHz. For the excitation pulses, we used the second harmonic of the fundamental beam at 400 nm. In order to minimize bimolecular effects, the excitation density was kept at $\approx$6 mJ cm^{-2}. White light generated with a 2 mm-thick sapphire plate was used as a probe in the visible region from 490 to 700 nm. For a spectrally resolved detection of the probe light, a spectrograph and CCD array were used. The chirp in the white light pulse was carefully taken into account during the analysis and evaluation of the obtained two-dimensional (wavelength and time) $\Delta T(\lambda,t)/T$ maps before extraction of the spectral and temporal data with homemade software. Overall, a temporal resolution of at least 150 fs was achieved for all excitation wavelengths.

Acknowledgements

DP acknowledges grants from MIUR (PRIN 2009-A5Y3N9) and INSTM-Regione Lombardia for partial support of this work. We thank Sara Benedini for early involvement in this work, and Prof. Mariella Mella for assistance in the VT NMR studies.

Notes and references

1 (*a*) L. Yao, S. Zhang, R. Wang, W. Li, F. Shen, B. Yang and Y. Ma, *Angew. Chem.*, 2014, **126**, 2151; (*b*) X. Wang, Y. Zhou, T. Lei, N. Hu, E. Q. Chen and J. Pei, *Chem. Mater.*, 2010, **22**, 3735; (*c*) W. Z. Yuan, P. Lu, S. Chen, J. W. Y. Lam, Z. Wang, Y. Liu, H. S. Kwok, Y. Ma and B. Z. Tang, *Adv. Mater.*, 2010, **22**, 2159; (*d*) H. Uoyama, K. Goushi, K. Shizu, H. Nomura and C. Adachi, *Nature*, 2012, **492**, 234; (*e*) Q. Liao, H. B. Fu and J. N. Yao, *Adv. Mater.*, 2009, **21**, 4153; (*f*) J. Y. Zheng, Y. L. Yan, X. P. Wang, Y. S. Zhao, J. X. Huang and J. N. Yao, *J. Am. Chem. Soc.*, 2012, **134**, 2880; (*g*) X. F. Duan, Y. Huang, R. Agarwal and C. M. Lieber, *Nature*, 2003, **421**, 241.

2 (*a*) Y. N. Hong, J. W. Y. Lam and B. Z. Tang, *Chem. Soc. Rev.*, 2011, **40**, 5361; (*b*) Z. Y. Zhang, B. Xu, J. H. Su, L. P. Shen, Y. S. Xie and H. Tian, *Angew. Chem., Int. Ed.*, 2011, **50**, 11654; (*c*) B. Wang, Y. C. Wang, J. L. Hua, Y. H. Jiang, J. H. Huang, S. X. Qian and H. Tian, *Chem.–Eur. J.*, 2011, **17**, 2647; (*d*) J. Mei, Y. Hong, J. W. Y. Lam, A. Qin, Y. Tang and B. Z. Tang, *Adv. Mater.*, 2014, **26**, 5429.

3 J. D. Luo, Z. L. Xie, J. W. Y. Lam, L. Cheng, H. Y. Chen, C. F. Qiu, H. S. Kwok, X. W. Zhan, Y. Q. Liu, D. B. Zhu and B. Z. Tang, *Chem. Commun.*, 2001, 1740.

4 (*a*) X. Y. Qi, H. Li, J. W. Y. Lam, X. T. Yuan, J. Wei, B. Z. Tang and H. Zhang, *Adv. Mater.*, 2012, **24**, 4191; (*b*) Z. Li, Y. Q. Dong, J. W. Y. Lam, J. X. Sun, A. J. Qin, M. Häußler, Y. P. Dong, H. H. Y. Sung, I. D. Williams, H. S. Kwok and B. Z. Tang, *Adv. Funct. Mater.*, 2009, **19**, 905; (*c*) F. Mahtab, Y. Yu, J. W. Y. Lam, J. Z. Liu, B. Zhang, P. Lu, X. X. Zhang and B. Z. Tang, *Adv. Funct. Mater.*, 2011, **21**, 1733; (*d*) G. Yu, S. W. Yin, Y. Q. Liu, J. S. Chen, X. J. Xu, X. B. Sun, D. G. Ma, X. W. Zhan, Q. Peng, Z. G. Shuai, B. Z. Tang, D. B. Zhu, W. H. Fang and Y. Luo, *J. Am. Chem. Soc.*, 2005, **127**, 6335.

5 J. Mei, N. L. C. Leung, R. T. K. Kwok, J. W. Y. Lam and B. Z. Tang, *Chem. Rev.*, 2015, **115**, 11718–11940.

6 R. Hu, J. L. Maldonado, M. Rodriguez, C. Deng, C. K. W. Jim, J. W. Y Lam, M. M. F. Yuen, G. Ramos-Ortiz and B. Z. Tang, *J. Mater. Chem.*, 2012, **22**, 232–240.

7 J. Wang, J. Mei, W. Yuan, P. Lu, A. Qin, J. Sun, Y. Ma and B. Z. Tang, *J. Mater. Chem.*, 2011, **21**, 4056–4059.
8 N. B. Shustova, B. D. McCarthy and M. Dincă, *J. Am. Chem. Soc.*, 2011, **133**, 20126–20129.
9 (*a*) X. Sun, Y. Liu, X. Xu, C. Yang, G. Yu, S. Chen, Z. Zhao, W. Qiu, Y. Li and D. Zhu, *J. Phys. Chem. B*, 2005, **109**, 10786; (*b*) Y. Shirota, *J. Mater. Chem.*, 2005, **15**, 75; (*c*) X. Y. Shen, W. Z. Yuan, Y. Liu, Q. Zhao, P. Lu, Y. Ma, I. D. Williams, A. Qin, J. Z. Sun and B. Z. Tang, *J. Phys. Chem. C*, 2012, **116**, 10541; (*d*) X. Y. Shen, Y. J. Wang, E. Zhao, W. Z. Yuan, Y. Liu, P. Lu, A. Qin, Y. Ma, J. Z. Sun and B. Z. Tang, *J. Phys. Chem. C*, 2013, **117**, 7334; (*e*) F. S. Kim, X. Guo, M. D. Watson and S. A. Jenekhe, *Adv. Mater.*, 2010, **22**, 478; (*f*) T. C. Lin, G. S. He and Q. Zheng, *J. Mater. Chem.*, 2006, **16**, 2490.
10 (*a*) E. Cariati, V. Lanzeni, E. Tordin, R. Ugo, C. Botta, A. Giacometti Schieroni, A. Sironi and D. Pasini, *Phys. Chem. Chem. Phys.*, 2011, **13**, 18005; (*b*) C. Coluccini, A. K. Sharma, M. Caricato, A. Sironi, E. Cariati, S. Righetto, E. Tordin, C. Botta, A. Forni and D. Pasini, *Phys. Chem. Chem. Phys.*, 2013, **15**, 1666.
11 T. Virgili, A. Forni, E. Cariati, D. Pasini and C. Botta, *J. Phys. Chem. C*, 2013, **117**, 27161.
12 M. M. Mróz, S. Benedini, A. Forni, C. Botta, D. Pasini, E. Cariati and T. Virgili, *Phys. Chem. Chem. Phys.*, 2016, **18**, 18289–18296.
13 C. Botta, S. Benedini, L. Carlucci, A. Forni, D. Marinotto, A. Nitti, D. Pasini, S. Righetto and E. Cariati, *J. Mater. Chem. C*, 2016, **4**, 2979–2989.
14 C. Hansch, A. Leo and R. W. Taft, *Chem. Rev.*, 1991, **91**, 165–195.
15 A. J. Zucchero, P. L. McGrier and U. H. F. Bunz, *Acc. Chem. Res.*, 2010, **43**, 397.
16 Y. M. Issa and W. H. Hegazy, *Synth. React. Inorg. Met.-Org. Chem.*, 2000, **30**, 1731–1746.
17 O. Attanasi, P. Filippone and A. Mei, *Synth. Commun.*, 1983, **13**, 1203–1208.
18 S. Zhu, B. Xu and J. Zhang, *J. Fluorine Chem.*, 1995, **74**, 167–170.
19 I. Shibuya, Y. Taguchi, T. Tsuchiya, A. Oishi and E. Katoh, *Bull. Chem. Soc. Jpn.*, 1994, **67**, 3048–3052.
20 B. A. Burkett, J. M. Kane-Barber, R. J. O'Reilly and L. Shi, *Tetrahedron Lett.*, 2007, **48**, 5355–5358.
21 The free energy barrier for the dynamic process ($\Delta G_c^{\ddagger}$) could be calculated using the coalescence method, where values for the rate constant k_c at the coalescence temperature (T_c) were calculated from the approximate expression $k_c = \pi(\Delta\nu)/2^{0.5}$, where $\Delta\nu$ is the limiting chemical shift difference (Hz) between the coalescing signals in the absence of exchange, and the Eyring equation was subsequently employed. See: (*a*) I. O. Sutherland, *Annu. Rep. NMR Spectrosc.*, 1971, **4**, 71–235. See also: (*b*) P. R. Ashton, S. E. Boyd, S. Menzer, D. Pasini, F. M. Raymo, N. Spencer, J. F. Stoddart, A. J. P. White, D. J. Williams and P. G. Wyatt, *Chem.–Eur. J.*, 1998, **4**, 299–310.
22 (*a*) M. Yu. Antipin, T. V. Timofeeva, R. D. Clark, V. N. Nesterov, M. Sanghadasa, T. A. Barr, B. Penn, L. Romero and M. Romero, *J. Phys. Chem. A*, 1998, **102**, 7222–7232; (*b*) K. Wang, Z. Wang and C. Yan, *Acta Crystallogr., Sect. E: Struct. Rep. Online*, 2001, **57**, o214–o215; (*c*) R. D. Gandour and F. R. Fronczek, *CSD Communication (Private Communication)*, 2015; (*d*) V. K. Gupta and R. A. Singh, *RSC Adv.*, 2015, **5**, 38591–38600.

23 (*a*) W. Ma, S.-Y. Zhang, J.-Y. Wu, Y.-P. Tian and H.-K. Fun, *Chin. J. Appl. Chem.*, 2003, **20**, 862; (*b*) Y. Jing and L.-T. Yu, *Acta Crystallogr., Sect. E: Struct. Rep. Online*, 2011, **67**, o1556.
24 F. H. Allen, O. Kennard, D. G. Watson, L. Brammer, A. G. Orpen and R. Taylor, *J. Chem. Soc., Perkin Trans. 2*, 1987, S1.
25 N. F. Phelan and M. Orchin, *J. Chem. Educ.*, 1968, **45**, 633.
26 M. H. Habibi, K. Barati, H. Etedali Habibadi, R. W. Harrington and W. Clegg, *Anal. Sci.*, 2008, **24**, x285–x286.
27 E. Solcaniova, P. Hrnciar and T. Liptaj, *Org. Magn. Reson.*, 1982, **18**, 55–57.
28 J. S. Yadav, D. C. Bhunia, V. K. Singh and P. Srihari, *Tetrahedron Lett.*, 2009, **50**, 2470–2473.
29 A. Szłap, S. Kula, U. Błaszkiewicz, M. Grucela, E. Schab-Balcerzak and M. Filapek, *Dyes Pigm.*, 2016, **129**, 80–89.
30 G. B. Kharas, S. M. Russell, V. Tran, Q. L. Tolefree, D. M. Tulewicz, A. Gora, J. Bajgoric, M. T. Balco, G. A. Dickey and G. Kladis, *J. Macromol. Sci., Part A: Pure Appl. Chem.*, 2008, **45**, 5–8.
31 J. S. A. Brunskill, A. De and G. M. Vas, *Synth. Commun.*, 1978, **8**, 1–7.
32 M. G. Wood, A. R. Smith and D. Judd, *US Pat.* No. 20030000130, 2003.
33 G. Charles, *Bull. Soc. Chim. Fr.*, 1963, **8–9**, 1559–1565.
34 J. Moreau, U. Giovanella, J.-P. Bombenger, W. Porzio, V. Vohra, L. Spadacini, G. Di Silvestro, L. Barba, G. Arrighetti, S. Destri, M. Pasini, M. Saba, F. Quochi, A. Mura, G. Bongiovanni, M. Fiorini, M. Uslenghi and C. Botta, *ChemPhysChem*, 2009, **10**, 647.
35 SMART, SAINT and SADABS, Bruker AXS Inc., Madison, Wisconsin, USA, 1997.
36 G. M. Sheldrick, *Acta Crystallogr., Sect. A: Found. Crystallogr.*, 2008, **64**, 112–122.
37 L. J. Farrugia, *J. Appl. Crystallogr.*, 2012, **45**, 849–854.
38 A. C. T. North, D. C. Phillips and F. S. Mathews, *Acta Crystallogr., Sect. A: Cryst. Phys., Diffr., Theor. Gen. Crystallogr.*, 1968, **24**, 351–359.
39 A. Altomare, M. C. Burla, M. Camalli, G. L. Cascarano, C. Giacovazzo, A. Guagliardi, A. G. G. Moliterni, G. Polidori and R. Spagna, *J. Appl. Crystallogr.*, 1999, **32**, 115–119.